

# Prediction of LC-VCOs' Tuning Curves with Period Calculation Technique

Zhangwen Tang, Jie He, Hongyan Jian, Haiqing Zhang, Jie Zhang, and Hao Min

ASIC & System State Key Laboratory, Fudan University, Shanghai 200433, P.R.China

Tel : +86-21-65642765\*819 Fax : +86-21-65644158

E-mail : {zwtang, jiehe, hyjian, hmin}@fudan.edu.cn

**Abstract**—This paper describes a new prediction method of tuning curves of a LC-tank voltage-controlled oscillator (VCO) with period calculation technique. With this period calculation technique, the prediction of oscillator tuning curves is more accurate compared with the traditional harmonic approximation. The theoretical analyses are experimentally validated with a CMOS complementary LC-tank VCO implemented in 0.35 $\mu\text{m}$  1P4M pure logic CMOS process.

## I. INTRODUCTION

The complementary cross-coupled negative- $G_m$  LC-tank oscillator is shown in Fig. 1, which employs both NMOS and PMOS cross-coupled pairs. Many published papers [1]-[4], have employed this type of LC-tank VCO, but oscillator tuning curves were obtained from SPICE simulations or measurements. The prediction of oscillator tuning curves is quite challenging due to highly nonlinear characteristics of varactors. A numerical method is shown in [2], but it is quite complex and time-consuming. The tuning curves must be numerically computed again if the bias current changes. M.Tiebout [3] and R.L.Bunch [4] et al. also found large-signal effects to the instantaneous capacitance of LC-tank, but their analyses were only qualitative. The recent papers in [5] and [6], introduced the notion of effective capacitance across the amplitude of oscillation, and presented an analytical solution to tank balance equation. Their approach was simple, but inaccurate since the second and higher order harmonics were neglected. Note that oscillating voltage in LC tank is not an ideal sinusoid [2], the effective capacitance of step-like varactors driven by a sinusoid is not the actual effective one in a true LC-tank VCO.

Recently, the design and modeling of on-chip MOS varactors is a hot topic. However, these researches are focusing on how to implement MOS varactors with high quality and large tuning range on standard Silicon CMOS technology. Few of them deal with the large-signal analyses, nonlinear effect to C-V curves and tuning curves of LC-tank. In Section II, the harmonic approximation method of the large-signal nonlinearity of varactors is briefly recalled, and the effective capacitance of LC tank is calculated. Section III investigates I-V locus of step-like MOS varactors in a serial LC-tank and predicts the tuning curves through the calculation of oscillating period of a LC tank in time domain. In Section IV, our prediction method in time domain is compared with the harmonic approximation in frequency domain. Lastly, the theoretical analyses are experimentally validated with a CMOS complementary LC-tank VCO.

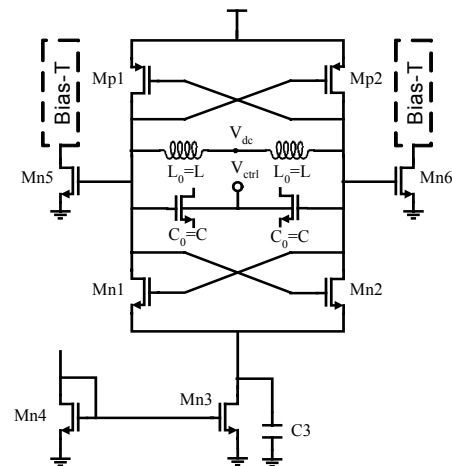


Fig. 1. CMOS complementary cross-coupled LC-tank VCO

## II. HARMONIC APPROXIMATION OF LC TANK IN FREQUENCY DOMAIN

Traditional small-signal analysis is not suitable for LC-tank oscillators with large-amplitude swings [2-5]. The large-signal effect must be considered. Thus, the effective capacitance calculation of LC-tank circuit is not a simple time-average process. In this section, we will briefly present how to calculate the effective capacitance through large-signal nonlinear analysis of varactors in a serial LC-tank circuit [2],[4]-[6].

The presence of on-chip inductors in Fig. 1 imposes that the dc value of differential oscillating voltages has to be a constant voltage  $V_{dc}$ . Neglecting the tank losses in on-chip inductors and varactors, the half circuit of LC-tank VCO can be considered as a serial LC-tank structure (Fig. 2(a))[6]. The oscillating voltage waveform can be represented as a Fourier series:

$$V_{out}(t) = V_0 + 2 \sum_{n=1}^{\infty} A_n \cos(n\omega t). \quad (1)$$

And, small-signal capacitance of varactors can be denoted as a Fourier series in time domain:

$$C_{ss}(V_C) = C_{ss}^{(0)} + 2 \sum_{n=1}^{\infty} C_{ss}^{(n)} \cos(n\omega t) \quad (2)$$

where  $C_{ss}^{(n)}$  is the Fourier coefficient at nth order harmonic.

Since serial LC-tank circuits must satisfy the Kirchhoff's laws, the inductor current must equal varactor current

$$I_L = I_C \Rightarrow \frac{1}{L} \int_{-\infty}^t V_L(t) dt = C_{ss}(V_C) \frac{dV_C}{dt}. \quad (3)$$

At the fundamental frequency, (3) must hold

$$\frac{A_1}{L\omega} = \omega \left\{ C_{ss}^{(0)} A_1 + \sum_{n=2}^{\infty} C_{ss}^{(n)} [(n+1)A_{n+1} - (n-1)A_{n-1}] \right\}. \quad (4)$$

Thus the effective capacitance  $C_{eff}$  is arrived

This work was supported in part by the Shanghai Science & Technology Committee, P.R.China under System-Design-Chip (SDC) program (NO. 037062019).

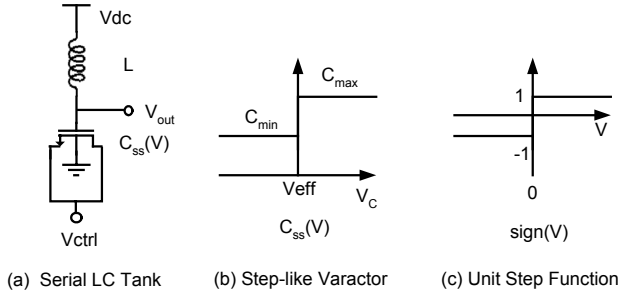


Fig. 2. Serial LC-tank and a step-like varactor

$$C_{eff} = \frac{1}{L\omega^2} = C_{ss}^{(0)} + \sum_{n=2}^{\infty} C_{ss}^{(n)} \left[ (n+1) \frac{A_{n+1}}{A_1} - (n-1) \frac{A_{n-1}}{A_1} \right]. \quad (5)$$

On the one hand, since oscillating amplitude varies with different control voltage, Fourier coefficients of varactors in (2) will change. On the other hand, the amplitude of  $n$ -th harmonic depends on the Fourier coefficients of varactors and effective capacitance. So the effective capacitance (5) is quite complex, if higher order harmonics could not be neglected. This is due to the large-signal and nonlinear effect of step-like varactors [2], [6].

### III. PERIOD CALCULATION OF LC-VCO

The technique of effective capacitance calculation is quite complex and inaccurate through Fourier series of varactors and oscillating voltage. In this section, we will directly derive the period of oscillating waveform, and then predict oscillator tuning curves in time domain.

Most varactors used in LC-tank VCOs are Inversion-MOS (I-MOS) and Accumulation-MOS (A-MOS). They are step-like capacitors (Fig. 2(b), and 2(c)), and have large nonlinearity. The small-signal capacitance is given by

$$C_{ss}(V) = \begin{cases} C_{max} & V \geq V_{eff} \\ C_{min} & V < V_{eff} \end{cases} \quad (6)$$

where  $V_{eff} = V_G - V_{ctrl} - V_{TH}$  is effective control voltage (ECV).

The half circuit of LC-tank VCOs is a serial LC tank shown in Fig. 2(a). The step-like varactor can also be mathematically represented as below,

$$C_{ss}(V) = \frac{1}{2}(C_{max} + C_{min}) + \frac{1}{2}(C_{max} - C_{min})\text{sign}(V - V_{eff}) \quad (7)$$

Fig. 3 shows oscillating voltage waveforms of a serial LC tank simulated in HSPICE. Each waveform consists of two segmental sinusoids with different sizes, which join at effective control voltage (ECV). With ECV from low to high, there exist four regions as below,

- 1) When  $V_{eff} \leq V_{dc} - A_{min}$ , the oscillating waveform is a sinusoid with a minimum amplitude  $A_{min}$  and minimum frequency  $\omega_{min}$ ;
- 2) When  $V_{eff} \geq V_{dc} + A_{max}$ , a sinusoid with a maximum amplitude  $A_{max}$  and maximum frequency  $\omega_{max}$ ;
- 3) When  $V_{dc} - A_{min} \leq V_{eff} \leq V_{dc}$ , two partial sinusoids join at ECV. One is over  $V_{eff}$  with the amplitude  $A_{min}$  and frequency  $\omega_{min}$ ; the other is below  $V_{eff}$  with the amplitude  $\theta A_{max}$  ( $\theta$  is an *ellipse similar factor, ESF*) and frequency  $\omega_{max}$ .
- 4) When  $V_{dc} \leq V_{eff} \leq V_{dc} + A_{max}$ , it consists of two segmental

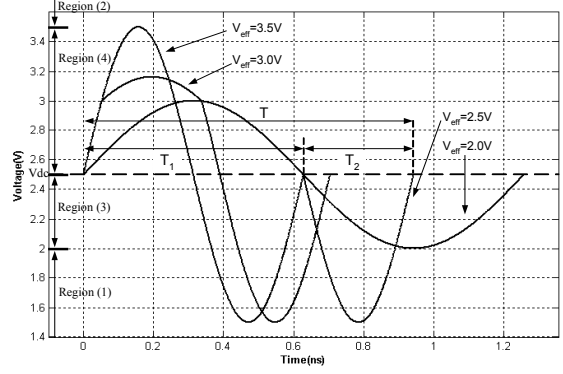


Fig. 3. Voltage waveforms of a varactor at different ECV

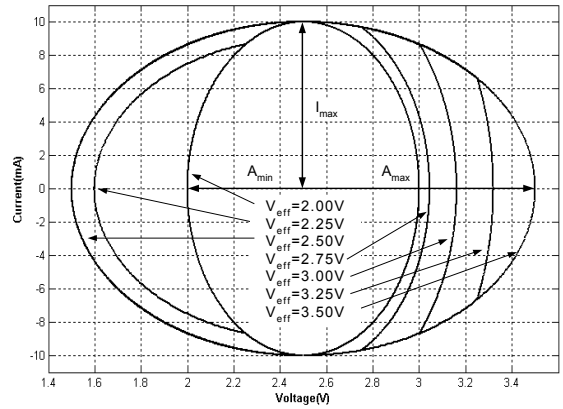


Fig. 4. I-V locus of a varactor

sinusoids joined at ECV. One is above  $V_{eff}$  with the amplitude  $\theta A_{min}$  ( $\theta$  is another ESF) and frequency  $\omega_{min}$ ; the other is below  $V_{eff}$  with the amplitude  $A_{max}$  and frequency  $\omega_{max}$ .

The I-V locus of a step-like varactor in a serial LC tank is shown in Fig. 4. It consists of two ellipses with different size joined at the ECV. The above four regions satisfy the following ellipse equations:

- 1) When  $V_{eff} \leq V_{dc} - A_{min}$ , the I-V locus holds

$$\left( \frac{V - V_{dc}}{A_{min}} \right)^2 + \left( \frac{I}{\omega_{min} C_{max} A_{min}} \right)^2 = 1; \quad (8)$$

- 2) When  $V_{eff} \geq V_{dc} + A_{max}$ , it holds

$$\left( \frac{V - V_{dc}}{A_{max}} \right)^2 + \left( \frac{I}{\omega_{max} C_{min} A_{max}} \right)^2 = 1; \quad (9)$$

- 3) When  $V_{dc} - A_{min} \leq V_{eff} \leq V_{dc}$ , two segmental sinusoids respectively hold

$$\left( \frac{V - V_{dc}}{A_{min}} \right)^2 + \left( \frac{I}{\omega_{min} C_{max} A_{min}} \right)^2 = 1, \quad \text{for } V \geq V_{eff},$$

$$\left( \frac{V - V_{dc}}{A_{max}} \right)^2 + \left( \frac{I}{\omega_{max} C_{min} A_{max}} \right)^2 = \theta^2, \quad \text{for } V \leq V_{eff}; \quad (10)$$

where ESF  $\theta$  satisfies  $A_{min}/A_{max} \leq \theta \leq 1$ . Especially when  $V_{eff} = V_{dc}$  and  $\theta = 1$ , it satisfies

$$I_{max} = \omega_{min} C_{max} A_{min} = \omega_{max} C_{min} A_{max} \quad (11)$$

where  $I_{max}$  is the maximum current in the inductor or varactor.

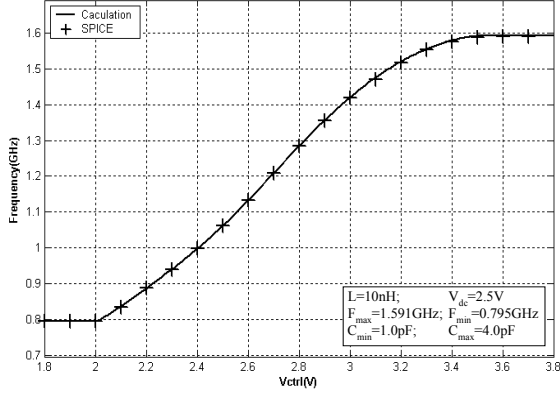


Fig. 5. Oscillator's tuning curves: simulated in SPICE, and calculated by (17) and (19)

4) When  $V_{dc} \leq V_{eff} \leq V_{dc} + A_{max}$ , two segmental sinusoids hold respectively

$$\left(\frac{V - V_{dc}}{A_{min}}\right)^2 + \left(\frac{I}{\omega_{min} C_{max} A_{min}}\right)^2 = \theta^2, \text{ for } V \geq V_{eff},$$

$$\left(\frac{V - V_{dc}}{A_{max}}\right)^2 + \left(\frac{I}{\omega_{max} C_{min} A_{max}}\right)^2 = 1, \text{ for } V \leq V_{eff}; \quad (12)$$

where ESF  $\theta$  satisfies  $1 \leq \theta \leq A_{max}/A_{min}$ .

The oscillating periods in the above four regions can be calculated mathematically.

1) When  $V_{eff} \leq V_{dc} - A_{min}$ , the oscillating period is

$$T = T_{max} = 2\pi\sqrt{LC_{max}}; \quad (13)$$

2) When  $V_{eff} \geq V_{dc} + A_{max}$ , the oscillating period is

$$T = T_{min} = 2\pi\sqrt{LC_{min}}; \quad (14)$$

3) When  $V_{dc} - A_{min} \leq V_{eff} \leq V_{dc}$ , the oscillating period is a sum of two intervals  $T = T_1 + T_2$ , shown in Fig. 3.  $T_1$  is the time on the first ellipse;  $T_2$  is the time on the second ellipse. At ECV, the voltage and current of varactor are  $V_{eff}$  and  $I_{eff}$ . From (11), (13) and (14), we obtain the amplitude ratio

$$\frac{A_{max}}{A_{min}} = \sqrt{\frac{C_{max}}{C_{min}}}. \quad (15)$$

Substituting (15) in (10) leads to the ESF  $\theta$

$$\theta = \sqrt{1 - \left(\frac{V_{eff} - V_{dc}}{A_{min}}\right)^2 + \left(\frac{V_{eff} - V_{dc}}{A_{max}}\right)^2}. \quad (16)$$

Thus, the oscillating period is

$$T = T_1 + T_2 = \frac{\frac{\pi}{2} + asin\left(\frac{|V_{eff} - V_{dc}|}{A_{min}}\right)}{\pi} T_{max} + \frac{\frac{\pi}{2} - asin\left(\frac{|V_{eff} - V_{dc}|}{\theta A_{max}}\right)}{\pi} T_{min}$$

$$= \frac{1}{2}(T_{max} + T_{min}) + \frac{1}{\pi} \left( asin\left(\frac{|V_{eff} - V_{dc}|}{A_{min}}\right) T_{max} - asin\left(\frac{|V_{eff} - V_{dc}|}{\theta A_{max}}\right) T_{min} \right); \quad (17)$$

4) When  $V_{dc} \leq V_{eff} \leq V_{dc} + A_{max}$ , The same as Case 3). Solving (12), we can obtain the ESF and oscillating period

$$\theta = \sqrt{1 - \left(\frac{V_{eff} - V_{dc}}{A_{max}}\right)^2 + \left(\frac{V_{eff} - V_{dc}}{A_{min}}\right)^2} \quad (18)$$

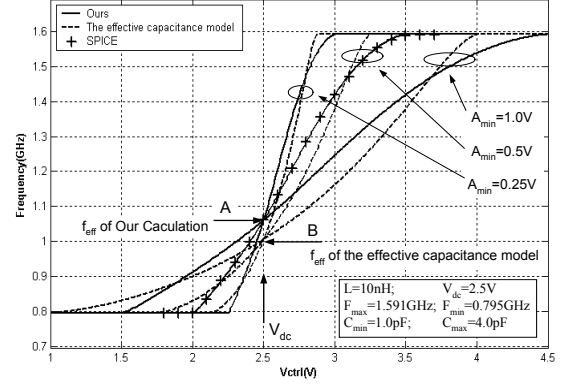


Fig. 6. Comparisons of tuning curves calculated by (17, 19) and by (20)

$$T = \frac{1}{2}(T_{max} + T_{min}) + \frac{1}{\pi} \left( -asin\left(\frac{V_{eff} - V_{dc}}{\theta A_{min}}\right) T_{max} + asin\left(\frac{V_{eff} - V_{dc}}{A_{max}}\right) T_{min} \right) \quad (19)$$

To validate the above method of oscillating period calculation, a serial LC-tank circuit in Fig. 2(a) is simulated in HSPICE. Its parameters are  $L=10\text{nH}$ ,  $C_{max}=4\text{pF}$ ,  $C_{min}=1\text{pF}$ , and  $A_{min}=0.5\text{V}$ . In Fig. 5, the cross line is the simulation result in HSPICE, and solid line is the calculation result from (17) and (19). The simulation agrees well with the calculation.

As the oscillator has a large signal swing (nearly full power supply), the oscillating period is interpolated between  $T_{max}$  and  $T_{min}$ . The resulting frequency-voltage (F-V) tuning curve, which is shown in Fig. 5, varies linearly with ECV in a range defined by the oscillation amplitude.

#### IV. COMPARISONS BETWEEN TIME-DOMAIN AND FREQUENCY-DOMAIN METHODS

The harmonic approximation in Section II is a frequency-domain method. Since the number of Fourier series in (1) and (2) is infinite, the neglect of high order harmonics in LC tank will induce inaccuracy to some extent. However, our new prediction of tuning curve in Section III is based on the period calculation technique. It is a time-domain method, which avoids the approximation inaccuracy.

Secondly, the period calculation technique is quite simple and convenient. The prediction method we proposed only requires the maximum and minimum capacitance ( $C_{max}$  and  $C_{min}$ ) and inductance  $L$ . At different current biases  $I_{bias}$ , the minimum amplitude  $A_{min}$  equals  $(4/\pi)I_{bias}R_{eq}$ , where  $R_{eq}$  is the equivalent parallel resistance of LC tank [1]. The maximum amplitude  $A_{max}$  can be calculated by (15). At different current biases, the tuning curves can be predicted immediately. However, the numerical solution based on the harmonic approximation in [2] should be time-consuming computed again, when bias current changes. Furthermore, Fourier coefficients of step-like varactors in (2) cannot be easily obtained by Fourier transform.

In [5], the prediction method of oscillator tuning curve with the effective capacitance is a simple case of harmonic approximation in Section II. Since the effective capacitance model neglected second and high order harmonics in (1), it

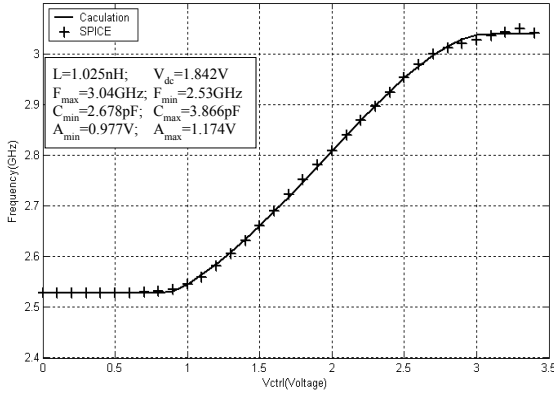


Fig. 7. F-V tuning curve of the simulation and calculation

only considered the effect of fundamental frequency to step-like varactor. Note that oscillating voltage in LC-VCOs is not an ideal sinusoid [2] [6], the effective capacitance in a true LC-VCO cannot be derived from a quasi-sinusoidal approximation. In [5], effective capacitance model is given by

$$C_{eff} = \frac{1}{2}(C_{max} + C_{min}) + \frac{1}{\pi}(C_{min} - C_{max}) \cdot \left( \text{asin}\left(\frac{V_{eff} - V_{dc}}{A}\right) + \left(\frac{V_{eff} - V_{dc}}{A}\right) \sqrt{1 - \left(\frac{V_{eff} - V_{dc}}{A}\right)^2} \right). \quad (20)$$

In order to compare with our prediction method, we use the average of  $A_{min}$  and  $A_{max}$  to approximate the parameter  $A$  in (20). Fig. 6 shows three groups of oscillator tuning curves calculate by (17), (19) and (20), at different minimum oscillating amplitudes ( $A_{min}=0.25V$ ,  $A_{min}=0.5V$ , and  $A_{min}=1V$ ). The solid lines are plotted by (17) and (19), and dash lines are the results of (20). When ECV voltage equals DC voltage  $V_{dc}$ , oscillating frequencies in (17), (19) and (20) respectively are  $F_{eff,A} = \frac{2F_{min} \cdot F_{max}}{F_{min} + F_{max}}$  (Point A in Fig. 6)

and  $F_{eff,B} = \frac{\sqrt{2}F_{min} \cdot F_{max}}{\sqrt{F_{min}^2 + F_{max}^2}}$  (Point B in Fig. 6).  $F_{eff,B}$  is always

small than  $F_{eff,A}$ . Thus compared to our prediction method, the effective capacitance model has more inaccuracy to some extent. The main reason is that the neglect of the second and higher order harmonics in (1) will lead to inaccuracy, which will increase when the ratio  $C_{max}/C_{min}$  increases.

## V. SIMULATION AND MEASUREMENT VALIDATIONS

The complementary cross-coupled negative- $G_m$  LC-tank oscillator in Fig. 1 has been implemented in TSMC 0.35 $\mu$ m 1P4M 3.3V pure logic CMOS process. The LC-tank VCO circuit is simulated in HSPICE. The tuning curve in Fig. 7 is obtained by the measurement of fundamental frequency at different ECVs. On-chip differential spiral inductor is 2.05nH, so the single-end inductor features 1.025nH. The maximum and minimum frequencies are 3.04GHz and 2.53GHz respectively, thus the  $C_{max}$  and  $C_{min}$  are 3.87pF and 2.68pF. And the DC voltage is 1.84V, the minimum amplitude is 0.98V, the maximum amplitude is 1.17V calculated by (15). In Fig. 7 and Fig. 8, the cross lines are results of the

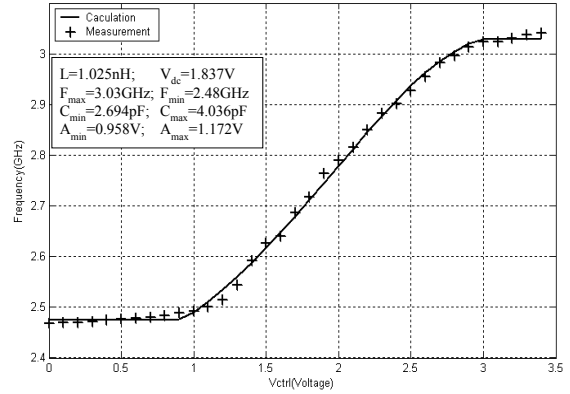


Fig. 8. F-V tuning curve of the measurement and calculation

simulation and measurement, and the solid lines are calculated by (17) and (19). The simulation and measurement agree well with the results obtained from the theoretical tuning curves' equation (17) and (19), over the entire tuning range.

## VI. CONCLUSION

Since the oscillating swing of LC-tank VCOs is large, the conventional small-signal analysis is not appropriate. The large-signal effect must be considered. However, the effective capacitance calculated by large-signal nonlinear analysis is complex and inaccurate. From the time domain, a new convenient period calculation technique is presented in this paper to predict the oscillator tuning curve. The simulation and measurement results agree well with the theoretical oscillator tuning curves over the entire tuning range.

## ACKNOWLEDGEMENTS

This work was supported in part by the Shanghai Science & Technology Committee, P.R.China under *System Design Chip* (SDC) program (NO. 037062019). The authors would also like to thank Chenbo Liu, Wei Yi, and Qifeng Jiang of Shanghai Research Center for Integrated Circuit Design, P.R.China, for the support of MPW service.

## REFERENCES

- [1] A. Hajimiri and T. H. Lee, "Design issues in CMOS differential LC oscillators," *IEEE J. Solid-State Circuits*, vol. 34, pp. 717-724, Feb. 1999.
- [2] S. Levantino, C. Samori, A. Bonfanti, S. L. J. Gierkink, A. Lacaita, and V. Boccuzzi, "Frequency dependence on bias current in 5-GHz CMOS VCOs: Impact on tuning range and flicker noise upconversion," *IEEE J. Solid-State Circuits*, vol. 37, pp. 1003-1011, Aug. 2002.
- [3] M. Tiebout, "Low-power low-phase-noise differentially tuned quadrature VCO design in standard CMOS," *IEEE J. Solid-State Circuits*, vol. 36, pp. 1018-1024, July. 2001.
- [4] R. L. Bunch, and S. Raman, "Large-signal analysis of MOS varactors in CMOS  $-G_m$  LC VCOs" *IEEE J. Solid-State Circuits*, vol. 38, pp.1325-1332, Aug. 2003.
- [5] E. Hegazi, and A. Abidi, "Varactor characteristics, oscillator tuning curves, and AM-FM conversion," *IEEE J. Solid-State Circuits*, vol. 38, pp.1033-1043, June 2003.
- [6] S. Levantino, C. Samori, A. Zanchi and A. L. Lacaita, "AM-to-PM conversion in varactor-tuned oscillator" *IEEE Trans. on Circuits and Systems-II, Analog and Digital Signal Processing*, vol. 49, pp.509-513, July 2002.